

Environmental source modelling to mitigate impact on marine life

Alex Goertz,^{1*} Jens Fredrik¹ Wisløff, Francis Drossaert¹ and Jaafar Ali¹ discuss how modelling the source output of marine airgun arrays can be used for planning marine mammal mitigation measures as part of marine seismic survey design and environmental permitting.

The impulsive signals emitted by seismic airguns are one of many sources of anthropogenic noise in the oceans. Concerns about potential adverse effects of anthropogenic noise on marine life have existed since the 1970s and have since triggered regulators to impose mitigation requirements in many jurisdictions worldwide. Such mitigation measures can include the definition of exclusion zones around sensitive areas, or the deployment of marine mammal observers (MMO). Sometimes, so-called sound source verification measurements are required to monitor sound levels in specific areas. In this paper, we describe how accurate forward-modelling of farfield signatures emitted from airgun arrays can be used to estimate the sound level of a marine seismic source as a function of distance. Results obtained from this modelling can be used for a variety of mitigation measures. These can include the planning of exclusion zones around sensitive areas, safety radii around seismic source vessels for the planning of MMO deployment, as well as the planning of so-called soft-start procedures, i.e., the process of ramping up the output of an airgun array by gradually adding individual guns over a sequence of shots.

The model that we employ to describe the pressure signature of an airgun is based on the theory of an oscillating spherical bubble that was first formulated by Kirkwood & Bethe (1942). Herring (1949) and Gilmore (1952) provided expressions of an equation of motion to describe the expansion and retraction of the bubble wall. Ziolkowski (1970) presented a method for the forward-calculation of airgun pressure pulses using this theory. Extensive research with a series of tests was carried out in the 1980s and early 1990s to further refine the model and apply the method for designing airgun arrays with optimal source output (e.g., Laws et al., 1990; Langhammer, 1994; Landrø, 1992; Strandenes & Vaage, 1992). Further overviews are provided by Parkes & Hatton (1986) and Dragoset (1990, 2000).

In this paper, we will first describe the source output in the frequency domain in relation to ambient noise levels in the ocean and the accuracy of the modelling over that frequency range. We discuss typical metrics to quantify the

strength of an underwater noise source as they are used in current regulatory frameworks. We present a workflow to obtain a measure of the source strength in the frequency band relevant for marine mammals from forward-modelled airgun signatures. We show how the workflow can be applied to the calculation of safety radii and exclusion zones, as well as the estimation of cumulative effects and the planning of startup procedures.

The spectrum of an airgun

Airguns were originally designed to provide a sharp pressure pulse of relatively broad frequency. In addition to the initial pressure pulse that is created when the air is released from the chamber, additional pulses are created by the oscillation of the bubble of air after it has been released. Since the period of the bubble oscillation is proportional to the cube root of the volume (e.g. Dragoset, 2000), the combination of airguns with different volumes into an array leads to suppression of the oscillating bubble pulses by superposition of the individual signatures from guns with different volumes. The initial pressure pulse is typically followed by the sea surface reflection, or ghost, which is a negative replication of the airgun signature with a time delay depending on the depth of the airgun. For the purpose of this paper, we are interested in the spectra of airguns and airgun arrays in comparison to the ambient acoustic noise. This is shown in Figure 1 where we compare measured signal and noise spectra from high-resolution gun calibration tests carried out in a deep Norwegian fjord (Mattson et al., 2012). Data from a single 30 cu.in airgun (grey and black lines) were measured 100 m below the surface and show a signal above the ambient noise level between 8 and 2000 Hz. The airgun was located at a depth of 6.35 m. We observe that the modelled signature (blue) fits the measured data very well up to 1 kHz. The modelling was carried out at a sampling rate of 0.5 m/s, hence the spectrum ends at 1 kHz. The ambient acoustic noise was measured using the same hydrophone just before the shot sequence.

The noise floor is at about 90 dB, representing very quiet conditions inside the fjord, and increases towards low frequencies due to wave and swell noise. A kink in the

¹ *Petroleum Geo-Services.*

* *Corresponding Author, E-mail: alexander.goertz@pgs.com*

Marine Seismic

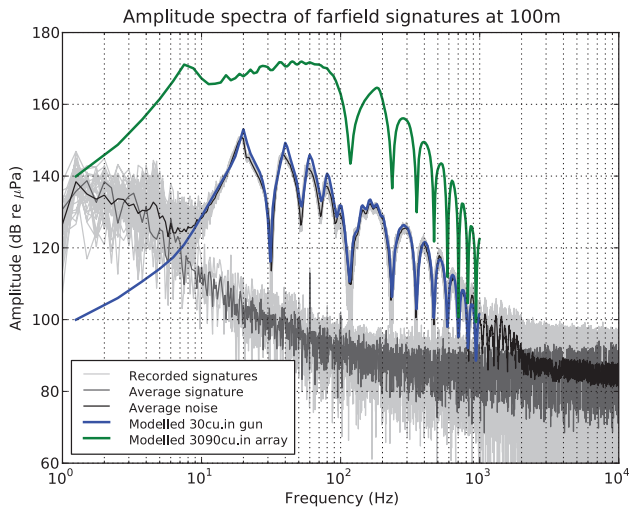
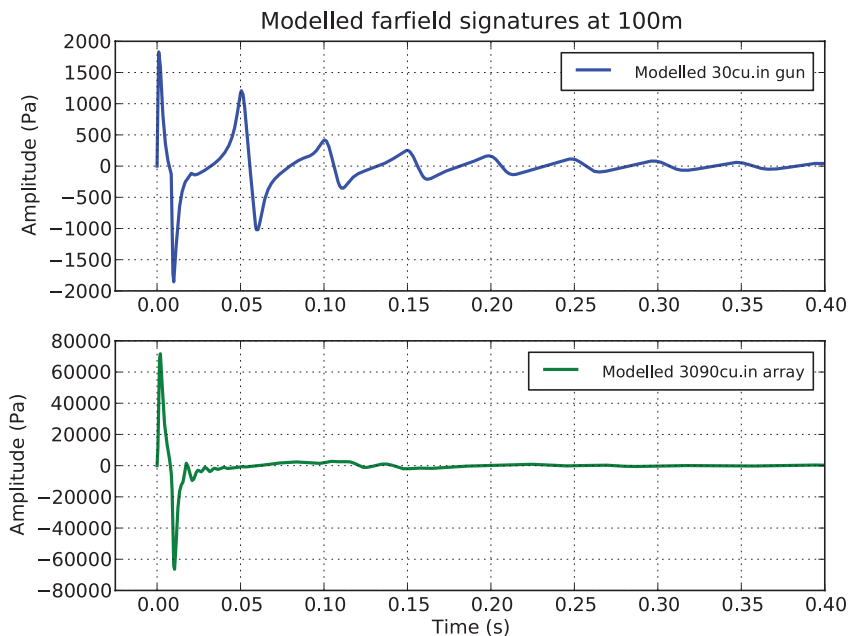


Figure 1 Grey lines show measured signal and noise spectra from a sequence of shots for a 30 cu.in gun under quiet conditions in a deep Norwegian fjord. Black lines are the average of all the individual shots. The blue line shows a modelled signature spectrum. The green line shows a modelled spectrum for a 3090 cu.in array.

average signal spectrum (black) at 2000 Hz indicates where the signal has decayed below the ambient noise level. The modelled spectrum for a 3090 cu. in gun array at the same distance of 100 m (green) shows a flatter spectrum below 100 Hz due to the suppression of the bubble pulse. The ambient noise level is reached at higher frequencies due to the generally higher output of the array compared to a single gun. A quantitative assessment of the signal levels with respect to the noise floor above 1 kHz is difficult since no high-frequency array measurements are available and the model does not include frequencies above 1 kHz.

Figure 2 Modelled time-domain signatures of the spectra shown in Figure 1. Top: Single 30 cu. in airgun at a depth of 6.35 m. Bottom: 3090 cu. in array at the same depth. Both signatures are modelled at 100 m vertically below the array. Note the 40-fold difference in scale of the vertical axis between the two plots.



Nevertheless, we observe a steeper decay of the array spectrum compared to the 30 cu.in single gun between 200 and 1000 Hz. High-frequency effects observed in data from a smaller linear source array are discussed in Landrø et al. (2011). Different physical effects at high frequencies would manifest themselves by a change in the slope of the high-frequency decay. Figure 2 shows the corresponding modelled time-domain signatures for the single 30 cu.in gun (blue) and the 3090 cu.in gun array (green).

Measuring mammal exposure levels

The energy of the signal is typically the best means to quantify the strength of a source to which marine life is exposed. Nevertheless, several – sometimes confusing and competing – measures and terminologies have been used in the past for quantification. In addition, it is often difficult to identify the contribution of one individual sound source in the presence of a myriad of other sound sources (most of them considered noise in this context), especially for stationary sound sources embedded in a non-stationary background signal. Here we will describe the two most popular measures that are unambiguously defined and widely applicable to a number of sound sources. These are the RMS pressure level (SPL_{rms}) and the sound exposure level (SEL). The RMS pressure level is a measure of the root-mean-square (RMS) amplitude of the signal in a chosen time window, in mathematical terms:

$$SPL_{RMS} = 20 \log_{10} \left(\sqrt{\frac{1}{T} \int P(t)^2 dt} \right)$$

The letter P stands for the pressure measured in μPa . The RMS pressure level is given in units of decibel (dB) with respect to 1 μPa . The RMS pressure level can be misleading if the ampli-

tude of the signal is strongly varying over the chosen time window. A better measure for transient signals is the sound exposure level (SEL), since it measures the energy in the signal in a specified window minus the background noise outside of this window:

$$SEL = 10 \log_{10} \left(\int_0^T P(t)^2 dt - \int_n^{n+T} P_n(t)^2 dt \right)$$

The signal window is typically chosen to be the time that comprises 5% to 95% of the cumulative energy. The noise window is typically a time window preceding the signal.

In addition to defining an unambiguous measure of the amplitude and energy in the sound signal, one needs to define the susceptibility of marine mammals to such signals in physical terms. Without going into biological details about possible behavioral and physiological impacts of sound, marine mammals (excluding pinnipeds in air) can generally be divided into four different functional hearing groups (Southall et al., 2007). These functional hearing groups are defined by the frequency band in which each group's species are most susceptible to sound exposure and hence have the highest likelihood of showing signs of behavioral reaction or physiological effects. Figure 3 shows the frequency response of bandpass filters representing the different functional hearing groups defined by Southall et al. (2007). For a realistic representation of the sound level a marine mammal is exposed to, any signal would have to be filtered accordingly before calculating SEL values. Note that only the low-cut of these filters is relevant for the exploration seismic frequency range.

Environmental modelling workflow

We have developed a workflow to arrive at estimates of sound exposures as a function of location that can be efficiently used for the planning of mitigation measures. In the

following, we refer to this workflow as 'environmental modelling'. The workflow is implemented in the Nucleus software and consists of the following steps:

- Modelling of farfield source signatures including close-range airgun interactions, ghost effects and array directivity.
- Calculation of geometrical spreading and intrinsic attenuation effects.
- Filtering of spreading-corrected signatures with a bandpass filter representing the desired functional hearing group (Southall et al., 2007).
- Calculation of RMS pressure level or SEL according to equations 1 and 2.
- Display of the attribute in map view or as a function of distance.

The individual steps of the workflow are displayed in Figure 4. The source modelling routine provides the time-domain farfield signature of an airgun array as a function of angle and distance. This signature is multiplied with an analytical geometrical spreading term that can be defined by the user on a sliding scale between cylindrical and spherical spreading. As the pressure wave propagates from the source, it will initially spread equally in all directions resulting in a spherical spreading with a loss of 20 dB per decade. The sea bed interaction will reflect back an increasing amount of energy as the incidence angle increases resulting in the larger distances being governed by cylindrical spreading, corresponding to a decay of 10 dB per decade. In reality, geometrical spreading will also depend on sound speed variations, sea bed properties and bathymetry. In many typical cases, spherical spreading is a valid approximation up to distances of 1.5 times the water depth, whereas cylindrical spreading can sometimes be a good first order approxima-

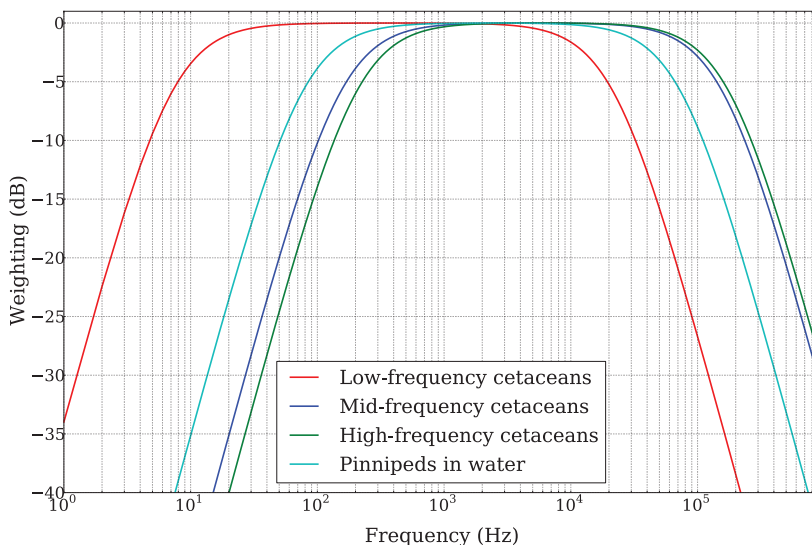


Figure 3 Bandpass filters (M-filters) defining the different functional hearing groups (reproduced from Southall et al., 2007).

Marine Seismic

tion for distances beyond several times the water depth (Urban, 2000).

At large distances and near-horizontal propagation, the amplitude of the propagating sound wave will be much smaller due to the destructive interference of the direct wave and the source ghost. This so-called Lloyd's mirror effect (e.g., Jensen et al., 2000) will under perfect circumstances (reflection coefficient of -1) give an additional 20 dB per decade loss in amplitude along a horizontal trajectory. The resulting radiation pattern, shown in Figure 5, illustrates how most of the energy is directed into the ground.

Application to specific mitigation measures

The resulting SEL or RMS pressure maps and graphs can be used in permitting and applied to the planning of specific mitigation measures. While a number of different applications are possible for the results of the outlined workflow, we restrict our discussion here to three which are straightforward to implement in practical acquisition scenarios and most often desired by regulators. We show example calculations in the following figures based on Southall's 'mid-frequency cetaceans' filter (Figure 3) and a semi-cylindrical propagation model.

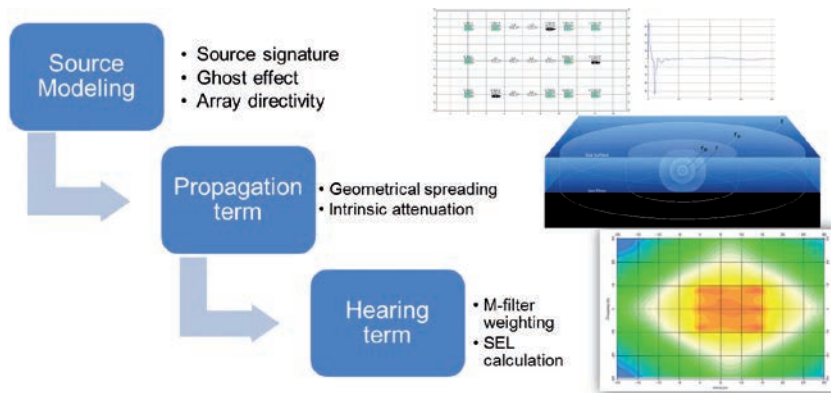
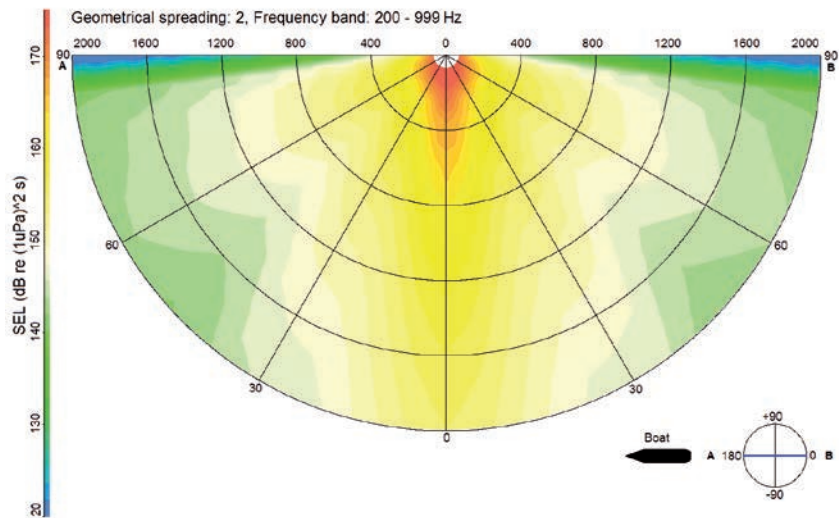


Figure 4 Illustration of the workflow that is applied to obtain a map of the sound exposure level around the airgun array from modelled array signatures.

Figure 6 shows a map of the calculated SEL values in a 6 x 6 km square around the source for the 3090 cu.in array. The inner contour at the centre of the plot has a SEL value of 198 dB re 1 $\mu\text{Pa}^2 \text{ s}$ and the second contour is 183 dB re 1 $\mu\text{Pa}^2 \text{ s}$. These represent Southall et al.'s (2007) injury and behavioural disturbance thresholds, respectively. This example suggests a 200 m safety radius outside of which the 183 dB limit (Southall et al., 2007) would not be exceeded. The survey geometry and acquisition plan may then be adapted accordingly. In addition, the size of the safety radius can have an influence on the planning of MMO deployment. Multiple MMO observation points or the deployment of a passive acoustic monitoring system (PAM) may be advisable, for example, if safety radii are large and visibility impairment is anticipated over that distance.

Another possible application is the estimation of the source output for individual array configurations in a soft-start procedure (Figure 7). In this process, the individual guns of an array are switched on sequentially in order to gradually ramp up the source output. The process is meant to disperse marine life away from the source with smaller source output before high levels are reached with the source at full force. In

Figure 5 Polar plot of array directivity for the 3090 cu. in array filtered with high-frequency cetacean band pass filter and applied spherical spreading. The radial axis displays distance from the source in metres, whereas the angular axis denotes the emergence angle from the array with 0° signifying vertical downward propagation and +/- 90° horizontal propagation. The large decay close to the surface is a result of Lloyd's mirror effect.



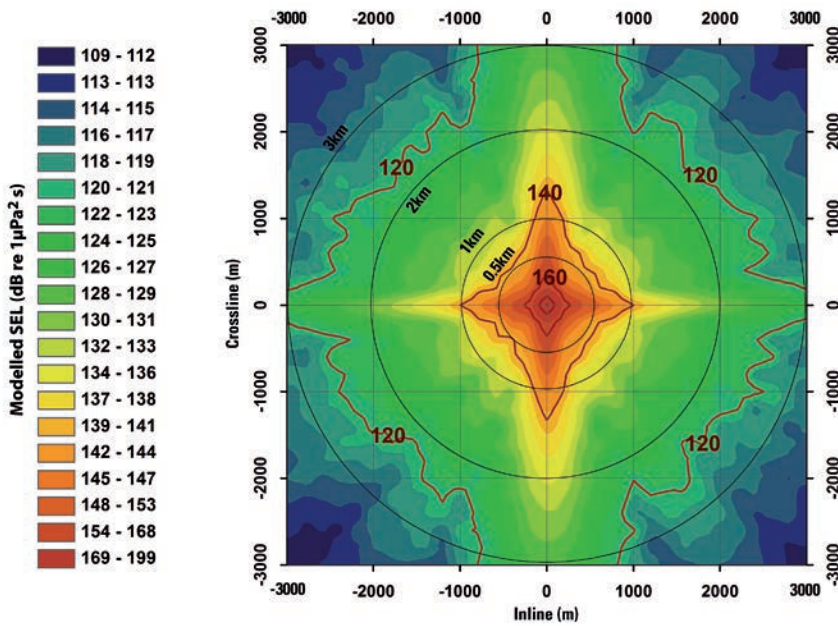
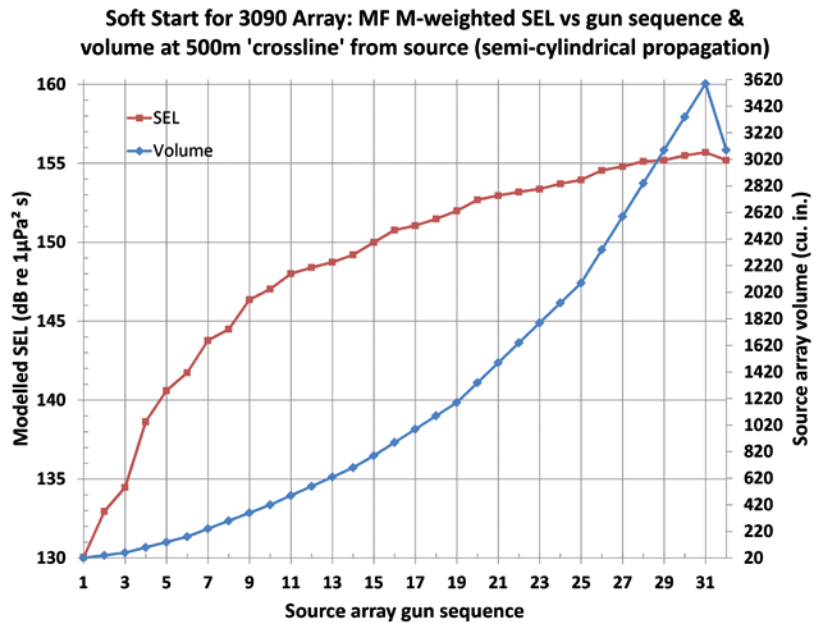


Figure 6 Map of sound exposure level (SEL) in a vicinity of 3 km around the source. Red contours indicate SEL in 20 dB intervals. Circles indicate radial distances from the source for orientation. Note the variation of the source directivity between inline and crossline offset. The SEL acoustic measure was computed at 1 m below the source.

Figure 7 Modelling of a soft-start procedure. Each sequence on the abscissa corresponds to an additional gun being switched on, starting with the smallest guns. Sequences 30 and 31 correspond to switching on the spare guns as well.



order to be effective, the source output of the individual array configurations in the sequence should be known to ensure that SEL values stay below regulated limits during the procedure. The different shapes of the volume (blue) and SEL (red) curves in Figure 7 is a result of the cube root dependence between volume and source output.

Sometimes the cumulative output of all shots of a particular sail line is requested (Figure 8). Here, the SEL value received by a stationary observing mammal is calculated and summed over a whole sail line at varying distances. Note that, although only ± 3 km profiles are shown in the figure, the cumulative effect was modelled for a whole sail line of

20 km. Individual SEL values are largest when the ship is abeam from the observer, here the centre of the sail line. Solid lines denote the summed cumulative SEL values for all shots of a sail line. As the ship recedes away from the observer, individual SEL values are subsequently smaller and little is added to the cumulative value. Note that the cumulative SEL values are dominated by the closest shots directly abeam from the observer where SEL values are largest.

Conclusion and outlook

Measures to mitigate the environmental impact of seismic surveys on marine mammals can become more effective if

Marine Seismic

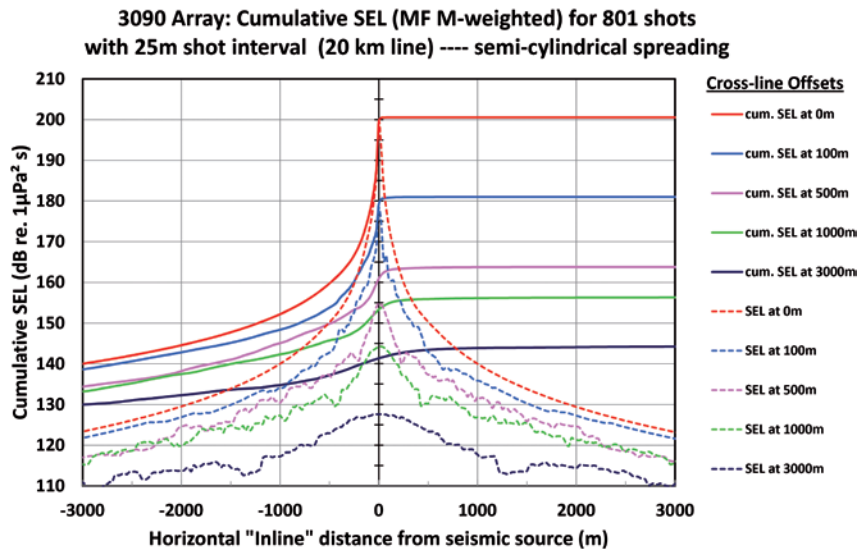


Figure 8 Individual (dashed) and cumulative (solid) SEL values received by a stationary observer for a sail line of shots passing the observer at different crossline offsets (colour). Largest individual SEL values are obtained when the ship is abeam. Cumulative values include shots up to ± 10 km.

the expected source output is modelled at the planning and permitting stage. An accurate estimate of the source output is provided by modelled far-field signatures that include the main physical effects around the source. We have shown that this physical model can describe the source output very accurately over the seismic frequency range up to 1 kHz.

We present a workflow for environmental modelling that is based on source signature modelling. The workflow provides a robust means to obtain key metrics for source output estimation in compliance with regulatory requirements, including SPL_{RMS} and SEL. Such estimates can be applied in numerous ways for the planning of specific mitigation measures. We have presented three such measures, spanning from the estimation of safety radii and exclusion zones to the planning of soft-start procedures and the estimation of cumulative SEL values along a sail line.

Current research focuses on the development of wave-equation based sound propagating modelling to improve the accuracy of the modelling at long ranges by way of including effects such as varying bathymetry, sound speed profiles, and seabed properties.

Acknowledgements

The acquisition of data shown in Figure 1 was funded through the Joint Industry Programme on E&P Sound and Marine Life. We are grateful to Petroleum Geo-Services for the permission to publish the results presented in this paper. Most figures in this paper were produced with Nucleus, a product of PGS.

References

- Dragoset, W.H. [1990] Air-gun array specs: a tutorial. *The Leading Edge*, 9(1), 24-32.
- Dragoset, B. [2000] Introduction to air guns and air-gun arrays. *The Leading Edge*, 19(8), 892-897.

- Gilmore, F.R. [1952] Growth and collapse of a spherical bubble in a viscous compressible liquid. *Report No. 264*, Hydrodynamics Laboratory, California Institute of Technology, Pasadena.
- Herring, C. [1949] Theory of the pulsations of the gas bubble produced by an underwater explosion. *Underwater Explosion Research*, 2, Office of Naval Research, Dept. of the Navy.
- Jensen, F., Kupermann, W., Porter, M. and Schmidt, H. [2000] *Computational ocean acoustics*. Springer Verlag, New York.
- Kirkwood, J.G. and Bethe, H.A. [1942] *The pressure wave produced by underwater explosion*. Office of Scientific Research and Development (OSRD) report No. 588.
- Landrø, M. [1992] Modelling of GI gun signatures. *Geophysical Prospecting*, 40, 721-747.
- Langhammer, J. [1994] *Experimental studies of energy loss mechanisms in air-gun bubble dynamics*. PhD thesis, Norges teknisk-naturvitenskapelige universitet (NTNU) Trondheim, Norway.
- Laws, R.M., Hatton, L. and Haartsen, M. [1990] Computer modelling of clustered airguns. *First Break*, 8(9), 331-338.
- Mattson, A., Parkes, G.E. and Hedgeland, D. [2012] Svein Vaage broadband air gun study. *The effects of noise on aquatic life, Advances in Experimental Medicine and Biology*, 730, 469-471.
- Parkes, G.E. and Hatton, L. [1986] *The marine seismic source*. D. Reidel Publishing Company, Dordrecht.
- Southall, B.L., Bowles, A.E., Ellison, W.T., Finneran, J.J., Gentry, R.L., Greene Jr, C.R., Kastak, D., Ketten, D.R., Miller, J.H., Nachtigall, P.E., Richardson, W.J., Thomas, J.A. and Tyack, P.L. [2007] Aquatic mammals – marine mammal noise exposure criteria: initial scientific recommendations. *Aquatic Mammals*, 33(4), 411-509.
- Strandenes, S. and Vaage, S. [1992] Signatures from clustered airguns. *First Break*, 10(8), 305-312.
- Urban, H.G. [2000] *Handbuch der Wasserschalltechnik, STN Atlas Elektronik*, Bremen.
- Ziolkowski, A.M. [1970] A method for calculating the output pressure waveform from an air gun. *Geophysical Journal of the Royal Astrological Society*, 21, 137-161.